Vibrational and electronic excitations in isotopically controlled diamonds

T. R. Anthony*, A. D. Alvarenga, M. Grimsditch†, Hyunjung Kim**, A. K. Ramdas**, S. Rodriguez** and R. Vogelgesang****

*GE Corporate Research and Development, Schenectady, NY 12309, USA
**Department of Physics, Purdue University, West Lafayette, IN 47907-1396, USA
†Argonne National Laboratory, Argonne, IL 60439, USA

Lattice vibrations of isotopically controlled single crystals of diamond ($^{12}C_{1-x}{}^{13}C_x$, $0 \le x \le 1$) are investigated with Raman, Brillouin, and Fourier transform infrared spectroscopy. The variation of the zone center optical phonon frequency and elastic moduli in the context of the virtual crystal approximation and zero-point motion; critical point frequencies as manifested in the two-phonon Raman and infrared spectra are addressed in these studies. The electronic infrared and Raman spectra of holes bound to substitutional boron acceptors in isotopically controlled diamonds show: (1) the Lyman transitions in which the bound states manifest host-related-self-energy shifts; (2) the spin-orbit splitting (Δ') of the 1s ground state into 1$s(p_{3/2})$ and 1$s(p_{1/2})$, 1$s(p_{1/2})$ being thermally populated; (3) a direct observation of the 1$s(p_{3/2}) \rightarrow$ 1$s(p_{1/2})$ transition as an electronic Raman at Δ', together with its isotopic effects.

DIAMOND can be viewed as an elemental group IV 'semiconductor' with a bandgap ~5.5 eV. When free from impurities, it is transparent from the ultraviolet to well into the microwaves, barring only the 2–6 μ range of multi-phonon absorption bands. The nearest neighbour, tetrahedrally coordinated, strong carbon–carbon sp^3 bonds make it the hardest terrestrial material; its unique lattice vibrational spectrum endows it with a very large Debye temperature and a thermal conductivity at room temperature surpassing even that of copper. This special combination of optical, mechanical, and thermal properties of diamond continues to command intense scientific interest and to generate significant technological applications[1,2]. The promise and the potential of a new generation of electronic devices based on diamonds have been well appreciated[3]. In this context, it is worth recalling the following statement made by Raman[4] in the concluding remarks of his 1930 Nobel Prize address: 'The case of the diamond, which has been investigated by Ramaswamy, Robertson, and Fox, and with especial completeness by Bhagavantam, is of special interest. Very surprising results have been obtained with this substance, which may be the pathway to a fuller understanding of the nature of the crystalline state'. Indeed, investigations on diamond feature prominently in Raman's researches throughout his scientific career[5].

In our contribution to this special issue of *Current Science* dedicated to the 70th anniversary of the discovery of the Raman Effect, we are honoured to present an account of our recent investigations on vibrational and electronic excitations in isotopically controlled diamonds exploiting infrared, Raman, and Brilliouin spectroscopy[6–10].

Experimental

Naturally-occurring diamonds have an isotopic composition corresponding to the natural abundance of carbon, viz. 98.9% ^{12}C and 1.1% ^{13}C. Diamonds containing nitrogen as a dominant impurity are classified as Type I. The relatively rare, nitrogen-free diamond is designated as Type IIa. Further, nitrogen-free but semiconducting diamond (p-type due to substitutional boron acceptors) is called Type IIb. Type IIb diamonds are *extremely* rare and exhibit remarkably low resistivities (5 to 10^5 Ωcm), whereas typical Type I and Type IIa diamonds have resistivities well in excess of 10^{18} Ωcm.

Until the first successful realization of single crystal diamond synthesis using the high-pressure–high-temperature (HPHT) technique[11] and the low temperature growth from the gaseous phase[12,13] by chemical vapour deposition (CVD), research on diamond was exclusively carried out on natural specimens. In the CVD process, the isotopic composition can be controlled by that of the gas employed; the isotopically controlled polycrystalline diamond can then be utilized in the HPHT technique to produce single crystals of $^{12}C_{1-x}{}^{13}C_x$ diamond with $0 \le x \le 1$ (ref. 14). To date, only p-type doping with substitutional group III boron impurities[15] has been successful, the impurity being introduced into the CVD diamond feedstock used in the HPHT growth[7]. In this manner we have access to single crystals of $^{12}C_{1-x}{}^{13}C_x$ diamonds throughout the composition range. In addition to Type IIb natural diamonds, a

man-made boron doped diamond with natural and ^{13}C composition is available to us.

Raman scattering experiments were performed with (1) a grating double monochromator (with a third for superior rejection of parasitic radiation) and photon counting electronics or (2) a CCD based multichannel triple spectrometer. A piezo-electrically scanned, multi-passed, tandem Fabry–Perot interferometer was employed for recording Brillouin spectra. The Raman and Brillouin spectra were excited with a variety of lines from an Ar^+ or a Kr^+ laser. A multi-scanned high resolution, Fourier transform spectrometer was used in infrared transmission experiments. Variable temperature optical cryostats enabled measurements of spectra with diamonds held at a temperature in the range 4.2 to 300 K.

Vibrational excitations

As is well known, inelastic neutron scattering from single crystals, investigated as a function of crystallographic direction, enables one to determine the frequencies of phonons (ω) with wavevectors ($\mathbf{q}$) spanning the entire Brillouin zone (BZ); indeed, phonon dispersion curves ($\omega(\mathbf{q})$) for diamond have been deduced in this manner by Warren *et al.*[16]. However, the significantly higher precision with which phonon frequencies can be determined and the feasibility of experiments even with specimens as small as 1 mm^3 make inelastic light scattering (Raman and Brillouin) and infrared spectroscopy very attractive for the study of phonons. In optical processes involving the creation (annihilation) of one phonon, i.e. in the first order Raman and infrared spectrum as well as in Brillouin scattering, only phonons near the zone center ($\mathbf{q} \sim 0$) can be excited (de-excited). The diamond lattice consists of two face-centered, interpenetrating, cubic (FCC) lattices displaced along the body diagonal by $(\frac{1}{4}a, \frac{1}{4}a, \frac{1}{4}a)$, a being the lattice constant. It belongs to the space group $O_h^7(F4_1/d\bar{3}2/m)$, the primitive unit cell containing two carbon atoms. The triply degenerate zone center optical phonon of F_{2g} symmetry is Raman allowed and infrared forbidden[17], since phonon features are subject to selection rules of non-vanishing polarizability (Raman) and electric dipole moment (infrared), respectively. In addition, wavevector conservation in two phonon processes restricts the participating phonons to $\mathbf{q}_i + \mathbf{q}_j \sim 0$. The second order spectra are quasi-continuous with peaks and slope discontinuities given by the joint density of states, in particular critical points (van Hove singularities) of the phonon dispersion curves.

It can be easily seen that the phonon frequencies ($\omega(\mathbf{q})$) in an isotopically-controlled diamond will scale as $M^{-1/2}$, where $M = xM_{13} + (1-x)M_{12}$, M_{12} and M_{13} being the masses of ^{12}C and ^{13}C, respectively; this is the *virtual crystal approximation* (VCA). One of the fundamental aspects of lattice dynamics, accessible in a crystal composed of light atoms as in diamond, is zero-point motion. In combination with the anharmonicity parameter (g_1), the F_{2g} frequency (ω_0), lattice parameter (a), and bulk modulus ($\mathcal{B}$) exhibit[6] an isotopic dependence displayed in Table 1.

The first order Raman spectrum of $^{12}C_{1-x}{}^{13}C_x$ diamond is displayed in Figure 1 *a* for x ranging from 0.992 to 0.001; the composition dependence of the zone center

Table 1. The F_{2g} frequency (Ω_0) lattice parameter (a_∞) and bulk modulus (B), in row 1, transform to ω_0, a and $\mathcal{B}$, reflecting the effects of zero-point motion and anharmonicity.

$$K_1 = k_1\left(1-\left[\hbar g_1^2/\left(8\sqrt{2}k_1^{5/2}M^{1/2}\right)\right]\right)$$

F_{2g} frequency	Lattice parameter	Bulk modulus
$\Omega_0 = \left[\frac{8(k_1+4k_2)}{3M}\right]^{1/2}$	a_∞	$B = (k_1/3a)$
$\omega_0 = \Omega_0\left(1-\frac{32\hbar g_1^2}{81M^3\Omega_0^5}\right)$	$a = a_\infty + \frac{\hbar g_1}{\sqrt{6}k_1^{3/2}M^{1/2}}$	$\mathcal{B} = (K_1/3a)$

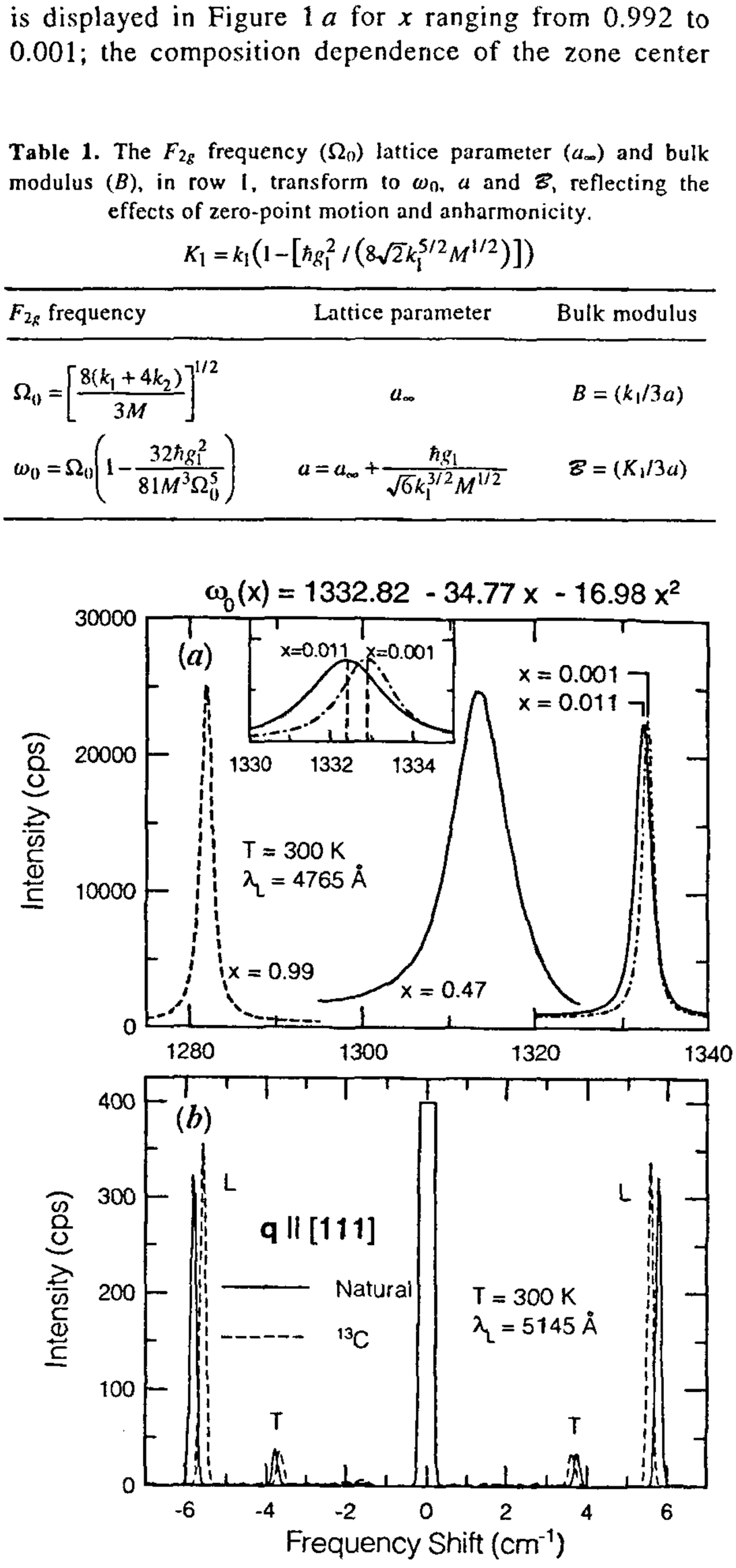

Figure 1. The Raman (*a*) and Brillouin (*b*) spectra of Type IIa $^{12}C_{1-x}{}^{13}C_x$ diamonds. The Brillouin spectra obtained with a large free spectral range of the tandem Fabry–Perot interferometer clearly show the signatures of longitudinal (L) and transverse (T) components (ref. 6).

Table 2. Elastic moduli c_{ij} and bulk modulus $\mathcal{B}$ of diamond (in units of 10^{12} dyne/cm^2)

x	c_{11}	c_{12}	c_{44}	$\mathcal{B}$
0.0	10.799(5)	1.248(10)	5.783(5)	4.432(8)
0.01105	10.804(5)	1.270(10)	5.766(5)	4.448(8)
0.992	10.792(7)	1.248(14)	5.776(7)	4.429(12)

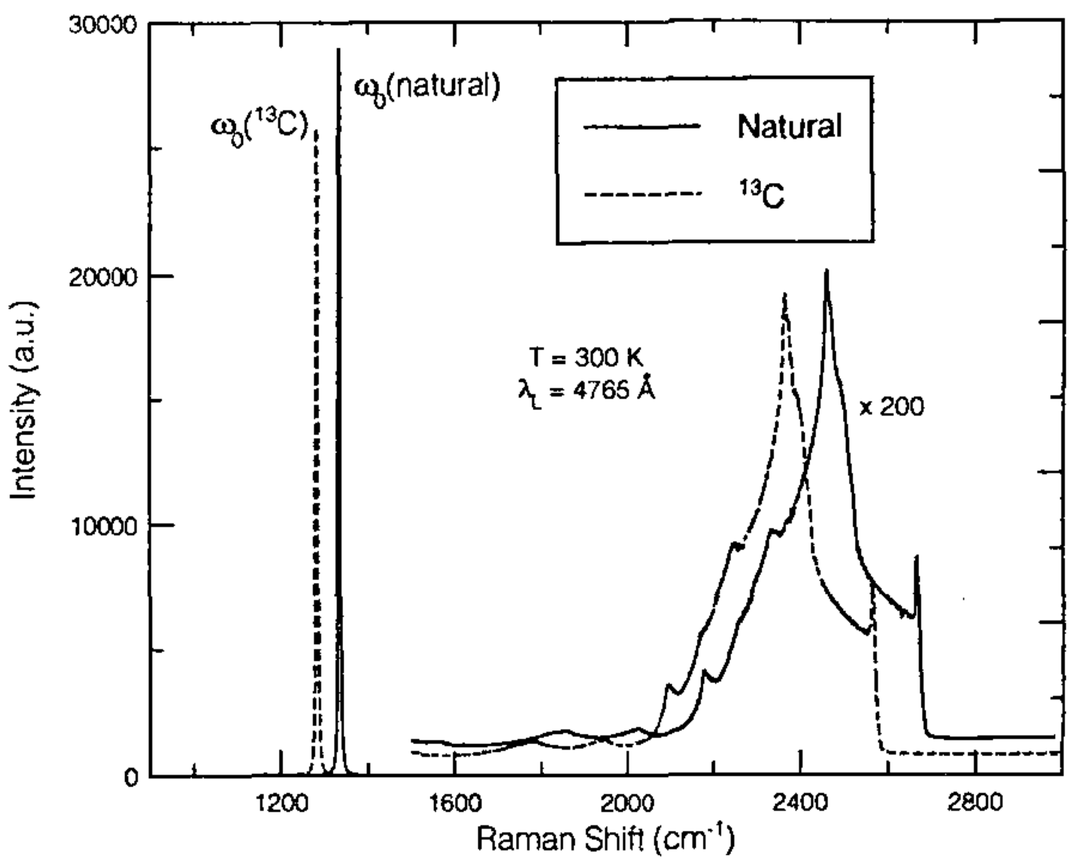

Figure 2. The Raman spectrum of a natural and a ^{13}C diamond. The spectra show the dominant first-order, Raman-active F_{2g} line and the significantly weaker, quasi-continuous, multi-phonon features (ref. 10).

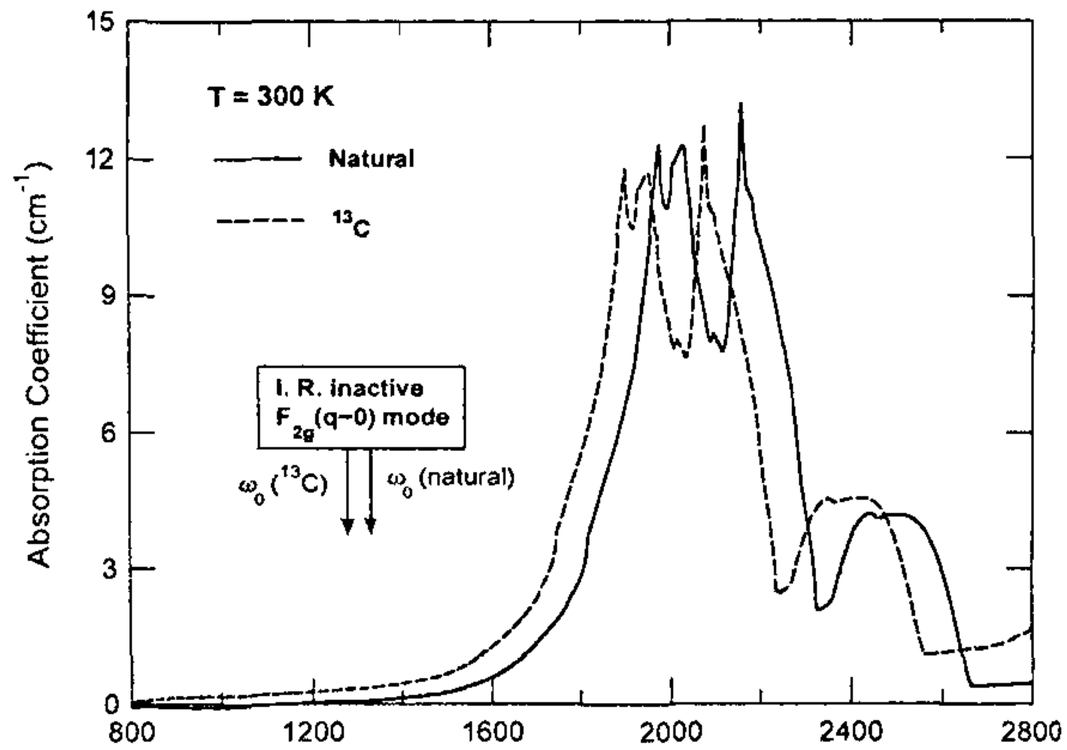

Figure 3. The multi-phonon features of a natural and a ^{13}C diamond in infrared absorption spectrum. Note the absence of the first-order line (ref. 10).

optical phonon frequency, ω_0 (x), reflects the contributions from zero point motion and anharmonicity, VCA and disorder effects. The experimental values 1332.8 cm^{-1} and 1281.6 cm^{-1} for $x = 0.001$ and 0.992, respectively, are consistent with those expected from considerations of zero-point motion, over and above VCA.

The Brillouin spectrum, recorded in the backscattering geometry for $\mathbf{q} \parallel [111]$ using the tandem Fabry–Perot interferometer, is shown in Figure 1 *b*; the longitudinal (transverse) Brillouin component yields sound velocities 1.860×10^6 (1.206×10^6) cm/s for $x = 0.001$ and 1.785×10^6 (1.158×10^6) cm/s for $x = 0.992$. On the basis of measurements on a number of samples, performed with the tandem feature omitted but with a free spectral range such that it produced a large order difference between the parent laser signature and the Brillouin shifted component, we were able to determine with high precision c_{11}, c_{12}, and c_{44}, the three independent elastic moduli for diamond with $x = 0.01105$ (natural), 0.001 and 0.992 (Table 2). The range in the bulk modulus $\mathcal{B} = [(c_{11} + 2c_{12})/3]$ in going from $x = 0$ to $x = 1$ is predicted to be 0.12%, just below the precision we were able to achieve in our measurements.

From a comprehensive analysis of multi-phonon features in (a) Raman spectra (Figure 2) recorded under diverse scattering geometries as well as different polarizations for the incident and scattered light, and in (b) infrared absorption spectra (Figure 3) using specimens with $x = 0.001$, 0.011, 0.992, we have identified a large number of combinations and overtones of phonons at the critical points in the BZ[10].

Electronic excitations

The ability to grow single crystals free of imperfections – be they lattice defects, or chemical impurities – followed by the controlled introduction of a desired imperfection is the prerequisite for a semiconductor to be significant in technology. While the HPHT and CVD techniques of diamond synthesis are milestones in this respect, the incorporation of shallow impurities (group III acceptors or group V donors) has been successful to date only for boron acceptors. The study of the bound states of donors and acceptors can be performed with extraordinary detail using infrared spectroscopy[18]. The Lyman spectrum and the associated Zeeman and piezospectroscopic effects of an acceptor or a donor yield the binding energies and the symmetries of the ground and excited states. To the extent the bound states are described in terms of the parameters of the band extremum with which they are associated, such a study is of clear value in the context of the properties of the host. Cyclotron resonance experiments[19] as well as transport measurements[20] have provided the Luttinger parameters and the spin–orbit splitting ($\Delta \approx 6$ MeV) characterizing the valence band maximum at the zone center. Motivated by these considerations, we have investigated the Lyman spectrum of boron acceptors in isotopically-controlled

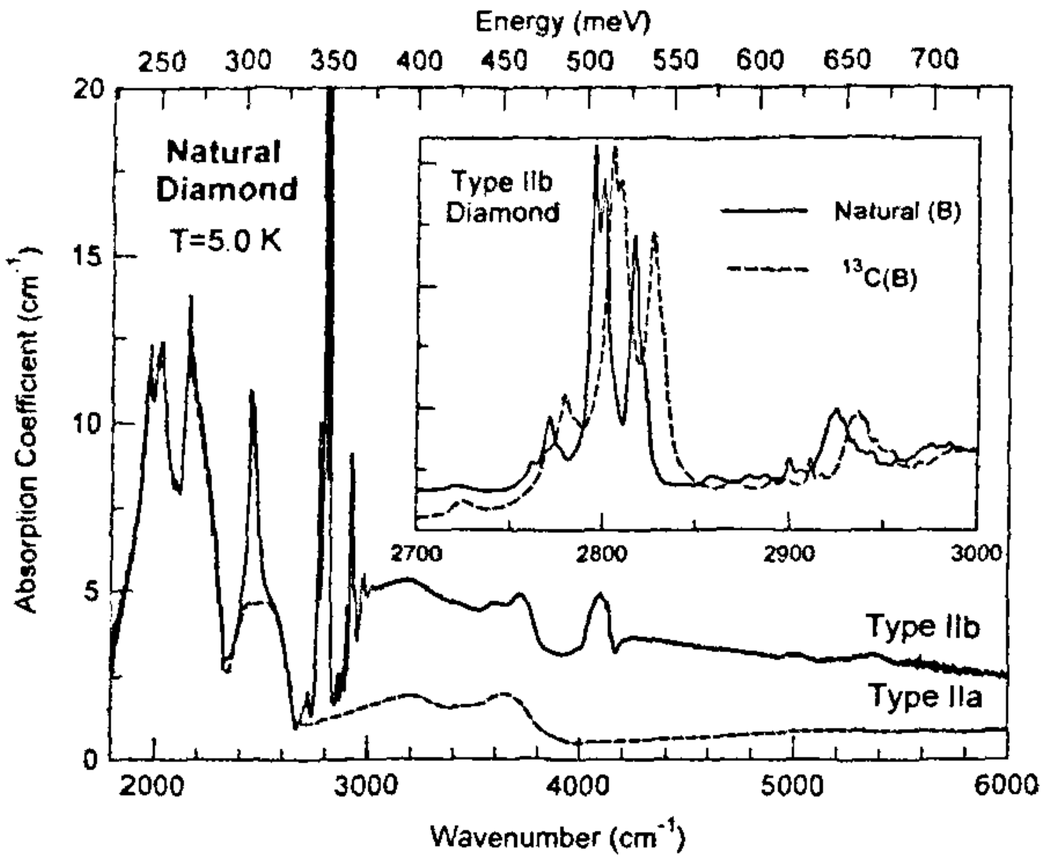

Figure 4. The absorption spectrum of a natural, Type IIa and of a Type IIb diamond, the latter showing the Lyman transitions of the boron acceptor. The inset shows the comparison of the Lyman spectrum of a natural and of a ^{13}C Type IIb diamond (ref. 7).

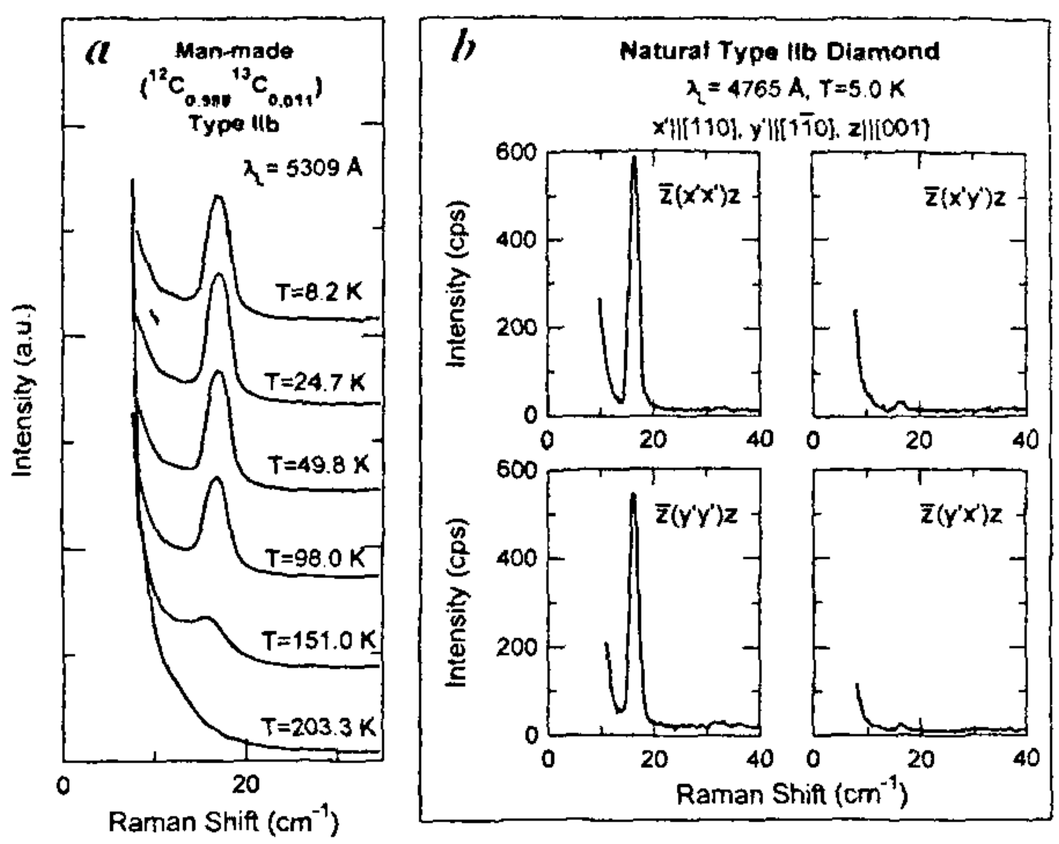

Figure 5. *a*, The $1s(p_{3/2}) \rightarrow 1s(p_{1/2})$ Raman transition of boron acceptors in a man-made Type IIb diamond with natural composition, recorded in backscattering along [001]. *b*, The polarization features of the Δ' Raman line of a natural Type IIb diamond in backscattering along z||[001]. The incident light is polarized along x'||[110] or y'||[110] and the scattered analysed along x' or y' (refs 8 and 9).

diamonds using Fourier transform infrared as well as Raman spectroscopy[7–9]. The selection rules for infrared and Raman transitions being different, the two techniques can be complementary.

In Figure 4 we display the absorption spectra of a natural Type IIa and boron-doped Type IIb diamonds in the spectral range 1800–6000 cm^{-1} recorded at 5.0 K. While both show identical intrinsic multi-phonon features, the spectrum of the Type IIb diamond clearly shows the characteristic sharp lines associated with the transitions of the acceptor bound hole from the ground to the various excited states[7]. The onset of the photoionization (~ 3000 cm^{-1}) persists well into the red and endows the boron-doped diamonds with its typical blue colour, the intensely blue Hope diamond being a striking example. The inset shows the comparison of the Lyman spectrum of a man-made ^{13}C boron-doped and that of a natural Type IIb specimen. While the spectra are strikingly similar even in minutest detail, the spectral lines of the acceptors in the ^{13}C diamond are unambiguously shifted by 3.1 to 11.8 cm^{-1} to *higher* energies. Since the acceptor in both natural and ^{13}C diamonds is boron, the small shifts strongly indicate that the acceptor states experience a central cell correction in ^{13}C diamond larger than that in the natural diamond. *We thus have a remarkable example of central cell corrections for the same substitutional acceptor but located in a host differing merely in its isotopic composition.*

When the infrared Lyman spectrum of the boron acceptors is studied as a function of temperature, new transitions appear at higher temperatures. The new lines can be ascribed to transitions originating from a higher lying, thermally populated, ground state ~ 2 MeV above the lower ground state responsible for the Lyman spectrum in Figure 4. Indeed, the 1*s* ground state of the acceptor bound hole is expected to show a spin-orbit splitting, Δ', into $1s(p_{3/2})$ and $1s(p_{1/2})$ corresponding to Δ of the valence band. It can be shown that the $1s(p_{3/2}) \rightarrow 1s(p_{1/2})$ transition is Raman active. Motivated by this prediction, we investigated the Raman spectrum of the boron-doped, isotopically-controlled diamonds[8].

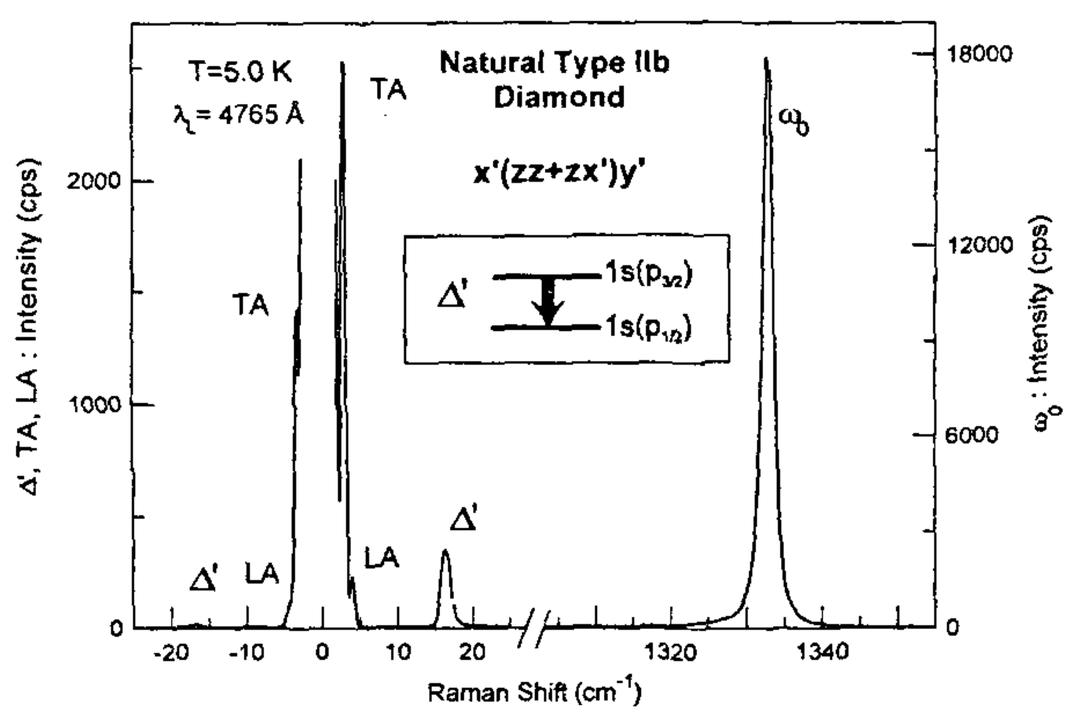

Figure 6. Comparison of the intensities of the Brillouin components (TA and LA), the Δ' line, and the zone center F_{2g} optical phonon at ω_0 in a natural Type IIb diamond, recorded in the right-angle scattering geometry $x'(zz + zx')y'$ (refs 8 and 9).

The electronic Raman spectrum of a man-made, boron-doped diamond of natural composition studied as

a function of temperature is shown in Figure 5 *a*. A new Raman line emerges as the temperature is decreased below ~150 K. The position of the line, 16.7(1) cm^{-1} = 2.07(1) MeV at 5.0 K, is entirely in agreement with that expected for the Raman active Δ' transition. Its disappearance at the elevated temperatures is obviously due to the thermal ionization of the boron acceptors, combined with its increased linewidth. Occurrence of the Δ' line as a Stokes/anti-Stokes pair and its appearance with the same shift when excited with different laser lines established that it is indeed a Raman line. The polarization characteristics of the Δ' Raman line, shown in Figure 5 *b* for backscattering, demonstrate that the corresponding polarizability tensor is predominantly Γ_5 in character, a feature fully substantiated by our calculations. The Δ' line in boron-doped ^{13}C diamond occurs at 16.2(1) cm^{-1} = 2.01(1) MeV at 5.0 K, once again highlighting the small, but spectroscopically accessible, effects of isotope-related self-energy shifts.

The Raman spectrum of natural Type IIb diamond at 5.0 K displayed in Figure 6 shows the Stokes/anti-Stokes pair of the Δ' line as well as the transverse (TA) and longitudinal (LA) Brillouin components, and the Stokes-shifted zone center optical phonon (ω_0). From the spectrum of the Raman lines of different origin, recorded under identical conditions, it has been possible to calibrate the intensities of Δ' and ω_0 and hence their absolute scattering cross-section.

1. *The Properties of Natural and Synthetic Diamond* (ed. Field, J. E.), Academic Press, San Diego, 1992.
2. *Properties and Growth of Diamond* (ed. Davies, G.), INSPEC, the Institution of Electrical Engineers, London, UK, 1994.
3. Geis, M. W. and Angus, J. C., *Sci. Am.*, 1992, **267**, 84–89.
4. *Scientific Papers of C. V. Raman*, *'Scattering of Light'* (ed. Ramaseshan, S.), Indian Academy of Sciences, Bangalore 1988, vol. I, p. 434.
5. *Scientific Papers of C. V. Raman, 'Optics of Minerals and Diamond'* and *'Physics of Crystals'* (ed. Ramaseshan, S.), Indian Academy of Sciences, Bangalore, 1988, vols IV and V.
6. Vogelgesang, R., Ramdas, A. K., Rodriguez, S., Grimsditch, M. and Anthony, T. R., *Phys. Rev.*, 1996, **B54**, 3989–3999.
7. Kim, H., Ramdas, A. K., Rodriguez, S. and Anthony, T. R., *Solid State Commun.*, 1997, **102**, 861–865.
8. Kim, H., Vogelgesang, R., Ramdas, A. K., Rodriguez, S., Grimsditch, M. and Anthony, T. R., *Phys. Rev. Lett.*, 1997, **79**, 1706–1709.
9. Kim, H., Vogelgesang, R., Ramdas, A. K., Rodriguez, S., Grimsditch, M. and Anthony, T. R., unpublished.
10. Vogelgesang, R., Alvarenga, A. D., Kim, H., Ramdas, A. K., Rodriguez, S., Grimsditch, M. and Anthony, T. R., unpublished.
11. Bundy, F. P., Hall, H. T., Strong, H. M. and Wentorf, R. H., *Nature*, 1955, **176**, 51–55.
12. Eversole, W. G., U.S. Patent Nos. 3030187 and 3030188, 1962.
13. Derjaguin, B. V., Fedoseev, D. V., Lukyanovich, V. M., Spitzin, B. V., Ryabov, V. A. and Lavrentyev, A. V., *J. Cryst. Growth*, 1968, **2**, 380–384.
14. Anthony, T. R. and Banholzer, W. F., *Diam. Relat. Mater.*, 1992, **1**, 717–726.
15. Chrenko, R. M., *Phys. Rev.*, 1973, **B7**, 4560–4567.
16. Warren, J. L., Yarnell, J. L., Dolling, G. and Cowley, R. A., *Phys. Rev.*, 1967, **158**, 805–808.
17. Nagendra Nath, N. S., *Proc. Indian Acad. Sci.*, 1934, **1**, 333–345. In this paper, the F_{2g} mode is shown to be the rigid oscillation of one FCC sublattice against the other. The group theoretical classification and the derivation of the F_{2g} frequency is given by Venkatarayudu, T., *Proc. Indian Acad. Sci.*, 1938, **A8**, 349–352.
18. Ramdas, A. K. and Rodriguez, S., *Rep. Prog. Phys.*, 1981, **44**, 1297–1387.
19. Rauch, C. J., *Phys. Rev. Lett.*, 1961, **7**, 83–84; *The Physics of Semiconductors*, The Institute of Physics and Physical Society, London, 1962, pp. 276–280.
20. Reggiani, L., Waechter, D. and Zukotynski, S., *Phys. Rev.*, 1983, **B28**, 3550–3555.

ACKNOWLEDGEMENTS. We acknowledge support from the National Science Foundation Grant No. DMR93-03186 at Purdue and from the US Department of Energy, BES Material Sciences (Grant No. W-31-109-ENG-38) at Argonne National Laboratory.